metals

MDPI

Article

Color-Metallographic Characterization of Alloyed White Cast Irons Ni-Hard Type

Milagrosa González Fernández de Castro, Yolanda Martín Álvarez, Juan José Moreno-Labella *, Miguel Panizo-Laiz and Benito del Río

Unidad Docente de Siderurgia, Escuela Técnica Superior de Ingenieros Industriales, Universidad Politécnica de Madrid, c/José Gutiérrez Abascal n°2, 28006 Madrid, Spain; m.gonzalez@upm.es (M.G.F.d.C.); ymartin@etsii.upm.es (Y.M.Á.); miguel.panizo.laiz@upm.es (M.P.-L.); benito.delrio@upm.es (B.d.R.)

* Correspondence: juanjose.moreno.labella@upm.es; Tel.: +34-91-067-70-53

Received: 8 May 2020; Accepted: 29 May 2020; Published: 1 June 2020

Abstract: The Ni-hard alloys white-cast irons are generally used for high wear work. Among them, those with better impact resistance because of its low carbon content compared to the rest of the family, are studied in this paper. One experimental technique of characterizing the metallic materials is the microstructural study. Several metallographic attacks intended to reveal qualitatively each microconstituent that forms the alloy, as well as the segregation and solidification structure of casting, are studied in this article. The use of color metallography is fundamental in this case to distinguish clearly the microconstituents. The main objective of this paper is to propose a series of attacks that identify each one of the microconstituents present in the alloy that has not been reported up to date.

Keywords: color metallography; microstructure; wear; alloyed white cast irons; Ni-hard; metallurgy

1. Introduction

Ferrous alloys have been studied for long. Nital-3 (3% solution of HNO_3 in alcohol) attack has been typically used for long, though it distinguishes between certain microconstituents neither in distribution nor in size [1,2], as it will be furtherly discussed. Mechanical properties and corrosion resistance are strongly dependent on the microstructure [3], so its proper identification is critical to understand the behavior of the material. In the case of Ni-hard alloys, little has been said about specific etchants that highlight the structure of these alloys [4,5]. Ni-hard alloys are classified according to standard [6], in the wear-resistant white-cast iron alloys. These white alloyed cast irons substitute the binary unalloyed white cast irons because of their higher tenacity and hardness. The percentages of carbon and chrome are variable depending on the mechanical requisites: the higher contents are used for high wear solicitations [7,8] and the lower contents are proper to acquire certain tenacity exigency [9]. This kind of ferrous cast alloys are widely used in mining, fluid transport, carbon industry, or metallurgy, among others [10,11], because of their advantages in fabrication and costs. The fabrication of elements for pulverizing mills is worth to be specially mentioned [12–14].

The microstructural evolution from the liquid state after cooling in sand mold begins with the solidification of austenite, which increases its carbon content as temperature decreases, up to reaching the eutectic temperature [15,16]. The solidification ends with the formation of the eutectic microconstituent. Its morphology is formed by a rounded-contoured matrix [17], made of M_3C-type carbides, that encircles the proeutectic austenite, the dispersed microconstituent. Both eutectic and proeutectic austenite are highly stable because of the high carbon and alloy contents in solution [18–20]. During the cooling between the eutectic and eutectoid temperature ranges, the proeutectic and eutectic

austenite segregates secondary globular-type carbides [18,19]. Depending on the cooling rate during the eutectoid interval, the austenite will eventually be partially transformed into pearlites (P), bainites (B), or martensites (M) since M_F (martensitic transformation end temperature) is typically much lower than the room temperature [1]. In the case of sand-mold cooling for medium thicknesses, the austenite will be partially transformed into martensite and isolated pearlitic zones. In slower cooling processes, segregation happens and the behavior of the last interdendritic fluid in solidification (LTF, last to freeze) is different owing to the high refractoriness of the austenite to be transformed [1].

Given the influence of the type, morphology, distribution, and quantity of microconstituents on the behavior in service of the cast iron [18,19], its identification is critical. The presence of austenite, pearlites, and bainites decreases the hardness and, therefore, the resistance to wear while increases the tenacity [9,21]. On the other hand, secondary carbides increase the hardness, while the initial and final martensitic transformation temperatures are increased when the austenite is destabilized because it contains less carbon and alloys in solution [7,22]. The microstructure of these alloys is well-known, but it is not easy to distinguish each of the constituents by metallurgical procedures [23,24]. Some of them, owing to its similarity in chemical composition and structure, are colored by the same etchants and are only distinguishable because of its color shade.

In this work, the characterization of the microconstituents that appear in Ni-hard alloys is systematized by selecting the proper selective reagents. This leads to a specific attack—or a sequence of them—to identify every single microconstituent. Although the separate use of the reagents for the characterization of iron-base alloys has already been described in the literature, the successive use of all of them for the study of Ni-hard alloys has not been reported. The traditional nital-3 etchant colors the austenite to brown tones and the pearlite to darker tones. Martensite remains unaltered as well as eutectic and secondary carbides, so it is necessary to study other attacks that identify these microconstituents [25,26].

2. Materials and Methods

Ni-hard cast-iron alloys have been used for more than fifty years in fields that require extreme hardness to work under high wear conditions. For metallic materials, an increase in hardness mostly imply embrittlement. Because of this fact, white cast irons found almost no application in industries, being replaced by alloyed cast irons [27]. To this purpose, four main types of Ni-hard alloy were developed [28,29]:

- Type 1: 3.0–3.6%C, 0.3–0.5%Si, 3.3–4.8%Ni, 1.5–2.6%Cr
- Type 2: <2.9%C, 0.3–0.5%Si, 3.3–5.0%Ni, 1.4–2.4%Cr
- Type 3: 1.0–1.6%C, 0.4–0.7%Si, 4.0–4.75%Ni, 1.4–1.8%Cr
- Type 4: 2.6–3.2%C, 1.8–2.0%Si, 5.0–6.5%Ni, 8.0–9.0%Cr

Besides, Ni-hard alloys can be modified through the addition of other elements, such as titanium [17], vanadium [30,31], molybdenum [32,33], manganese [34] or boron [35]. Wear resistance is related to the chemical composition and the microstructure of the alloy. Wear rate sinks as carbon content decreases for both cast irons and steels—in absence of graphite. Regarding the microstructure, the higher percentage of martensite, the more resistant the alloys are. Besides, the presence of eutectic carbides is more beneficial than the secondary ones, because the latter may be detached from the matrix [18,19].

In this study, the microstructural characterization has been done by optical microscopy of the higher tenacity Ni-hard (EN-GJN-HB480) whose composition according to emission spectrographic analysis is 2.75–2.98%C; 0.5–0.67%Si; 0.50–0.77%Mn; 0.04–0.06%P; 0.02–0.06%S; 4.17–4.50%Ni and 1.82–2.00%Cr. The test pieces were molded in chemical sand and molten in an induction furnace of intermediate frequency (3 kHz) AJAX GUINEA, in a 200 kg crucible, from a temperature of 1340 °C. The specimen for the metallographic analysis was obtained by cutting with a metallographic metal cutting machine of 30 mm diameter round pieces. The characterization has been done in the as-cast

condition. After sectioning, the pieces were encapsulated in a metallographic mounting press with NXMET high-quality phenolic resin. Once they are encapsulated, they were ground and polished before being attacked.

Attacks were performed with the reagents in Table 1. For this work, the sequence of attacks is:

- Attack 1: Marshall reagent for 5 s at room temperature
- Attack 2: Marshall reagent for 25 s at room temperature
- Attack 3: Marshall reagent for 60 s at room temperature
- Attack 4: Attack 3 + 5% ammonium persulfate at room temperature
- Attack 5: Attack 4 + Kalling N°1
- Attack 6: Murakami hot reagent
- Attack 7: Murakami reagent at room temperature
- Attack 8: Klemm reagent for 20 s
- Attack 9: Nital-3 at room temperature
- Attack 10: Marble reagent
- Attack 11: Picral reagent
- Attack 12: Vilella reagent for 20 s

Table 1. Reagents used.

Reagent	Composition
Murakami [36]	10 g $K_3[Fe(CN)_6]$, 10 g KOH and 100 mL H_2O
Klemm [37,38]	50 mL of H_2O, $Na_2S_2O_3$ until saturation, and 1 g of $K_2S_2O_5$
Marble [39]	10 g $CuSO_4$, 50 mL of HCl and 50 mL of H_2O
Marshall [40]	28 mL of 5% oxalic acid, 80 mL of H_2O and 4 mL of 30% H_2O_2
Nital-3 [24]	3% HNO_3 in ethyl alcohol
Ammonium persulfate [41]	5 g of $(NH_4)_2S_2O_8$ and 100 mL of H_2O
Kalling N°1 [42]	1.5 g of $CuCl_2$, 33 mL of H_2O, 33 mL of HCl and 33 mL of ethanol
Picral [24]	100 mL of Ethanol and 4 g of $C_6H_2OH(NO_2)_3$
Vilella [42]	1 g of $C_6H_2OH(NO_2)_3$ and 5 mL of HCl and 100 mL of ethanol

For these attacks, etchants, reaction times, and temperatures were chosen according to specialized studies [1,5,26,43,44]. The key point is to minimize the etching time and the temperature not to burn the microstructure. This would induce the darkening of the microconstituent instead of its identification. It is preferable to accomplish a series of short attacks, checking the results after each one, instead of attacking the sample for long.

3. Results

The microconstituents that can be present in the alloy are proeutectic austenite (APE), martensite (M), pearlite (P), secondary carbides (CS), eutectic carbide (CE), and eutectic (E) [10]. Contrary to other ferrous alloys, in Ni-hard works, it is not common to distinguish between pearlites and bainites because they show almost the same pernicious properties, so the term "pearlite" actually refers to any biphasic aggregate that comes from the diffusive decomposition of the austenite in ferrite and cementite. However, many structures are distinguished as the decomposition temperature—as well as the thickness of these lamellas—is lowered: pearlite, sorbite, troostite, upper bainite, and lower bainite [1,16]. Generally, the thinner the lamellas are, the more resistant and brittle the biphasic constituent is. Though there are plenty of possibilities among the etchants to identify the microconstituents of these alloys, the selected attacks are focused on unequivocally highlight any of them.

3.1. Attack 1—Marshall Reagent for 5 s at Room Temperature

With this attack during 5 s of immersion, the edges of the eutectic carbides can be observed, and the proeutectic austenite grains are delimited. Inside the proeutectic grains of austenite, needles of an undetermined constituent start to be spotted. These needles may correspond to the upper bainite as well as martensite (Figure 1).

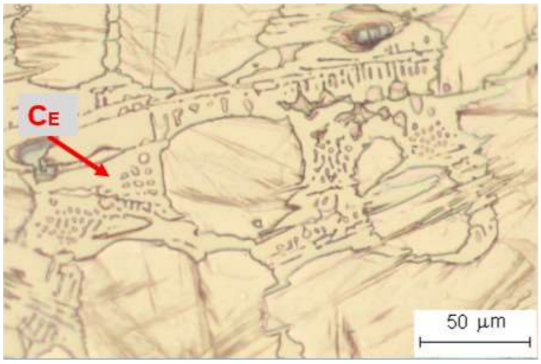

Figure 1. Marshall reagent for 5 s at room temperature (200×).

3.2. Attack 2—Marshall Reagent for 25 s at Room Temperature

By prolonging the previous attack, more contrast is gotten in the edges of the eutectic carbides and the proeutectic austenite. Pearlite areas (P) are observable inside the proeutectic grains in 500×, in the shape of dark laminar areas (Figure 2).

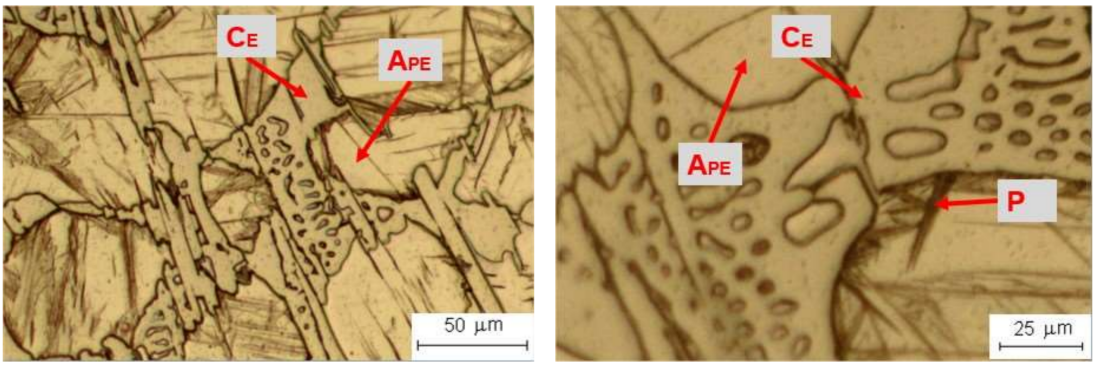

(**a**) (**b**)

Figure 2. Marshall reagent for 25 s at room temperature: (**a**) general view at 200×;(**b**) detail at 500×.

3.3. Attack 3—Marshall Reagent for 60 s at Room Temperature

Prolonging the reagent time, the contrast of pearlitic zones and the definition of martensite needles enhance. The typical morphology of the transformed eutectic formed by the carbide matrix, the retained austenite, the pearlite, and the martensite needles are now perfectly distinguishable. Martensite is attacked is a slighter way, but its characteristic disposition at 60° is observable and makes it distinguishable from pearlites (Figure 3).

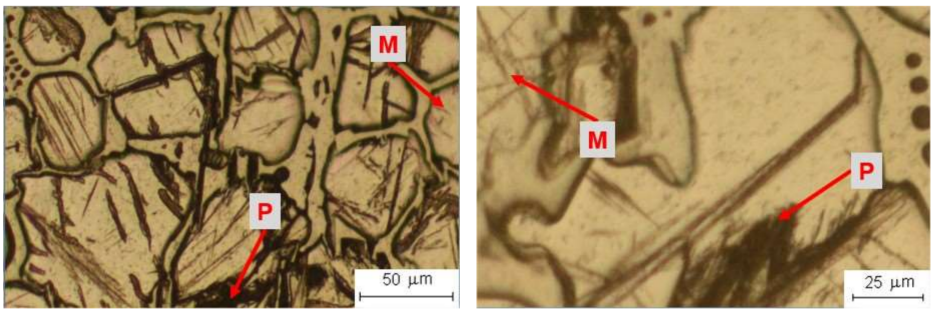

(**a**) (**b**)

Figure 3. Marshall reagent for 60 s at room temperature: (**a**) general view at 200×; (**b**) detail at 500×.

3.4. Attack 4—Attack 3 (Marshall Reagent for 60 s at Room Temperature) + 5% Ammonium Persulfate at Room Temperature

After attacking with ammonium persulfate, the austenite inside the proeutectic constituents is bluish-colored, revealing the dark-brown pearlite and the martensite needles in a lighter-brown tone. The presence of white carbides can be observed inside the proeutectic grains. Once again, the microstructure typical of the eutectic is identified. This attack highlights the austenite, and the intragranular carbides—inside the grains—remain unaltered (Figure 4).

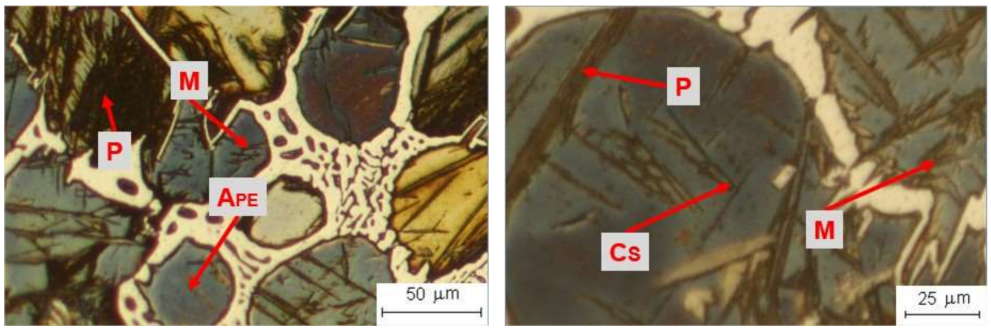

(**a**) (**b**)

Figure 4. Attack 3 (Marshall reagent for 60 s at room temperature) + 5% ammonium persulfate at room temperature: (**a**): general view at 200×; (**b**) detail at 500×.

3.5. Attack 5—Attack 4 (Marshall Reagent for 60 s at Room Temperature, 5% Ammonium Persulfate at Room Temperature) + Kalling N°1

Attack 4 + Kalling N°1 transforms the blue color of the retained austenite, because of the ammonium persulfate reaction, into light brown and turns even darker the martensite needles. The secondary carbides inside the proeutectic grains are revealed much more clearly (Figure 5).

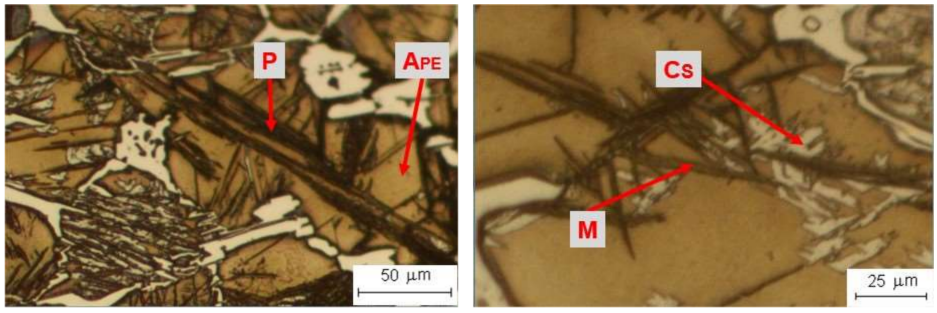

(**a**) (**b**)

Figure 5. Attack 4 (Marshall reagent for 60 s at room temperature, 5% ammonium persulfate at room temperature) + Kalling N°1: (**a**) general view at 200×; (**b**) detail at 500×.

The presence of secondary carbides is limited because these Ni-hard alloys have few carbide-forming elements and low carbon content. Despite this fact, they are segregated during continuous cooling between eutectic and eutectoid temperatures after solidification.

3.6. Attack 6—Murakami Hot Reagent

To only color the carbides of the eutectic, hot Murakami reagent accelerates the reaction. Bluish coloration of the eutectic carbide network and martensite needles is observed. Small areas with the same coloration are observed inside the proeutectic grains, which coincide with the secondary carbides (Figure 6).

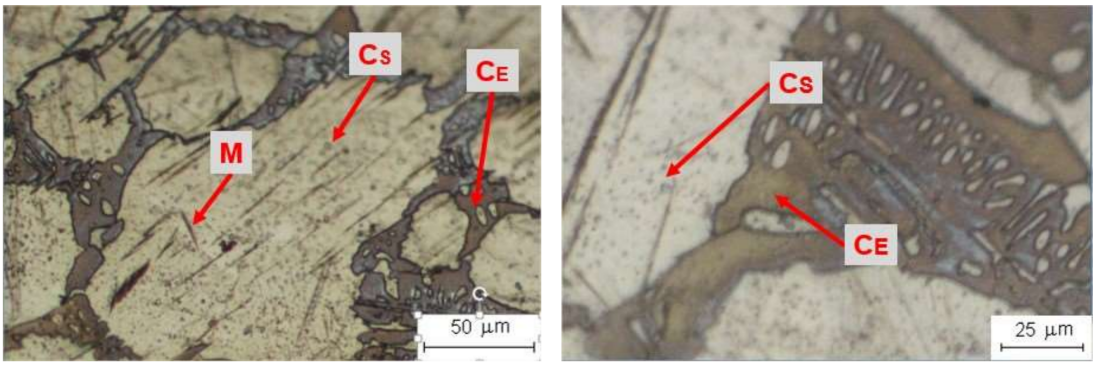

(**a**) (**b**)

Figure 6. Murakami hot reagent: (**a**) general view at 200×; (**b**) detail at 500×.

3.7. Attack 7—Murakami Reagent at Room Temperature

In addition to the matrix of eutectic carbides, the Murakami reagent at room temperature highlights dark areas referring to the carbon segregation in the cast iron. Large amounts of small carbides are identified inside and outside the proeutectic grain (Figure 7).

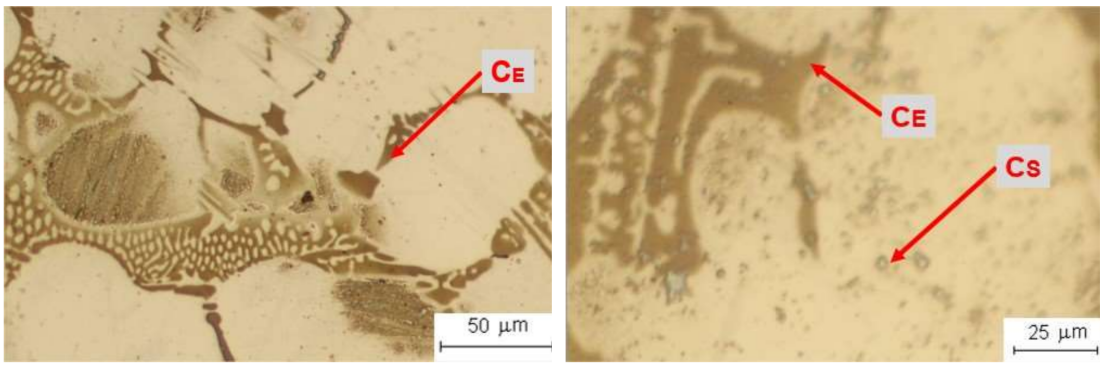

(**a**) (**b**)

Figure 7. Murakami reagent at room temperature: (**a**) general view at 200×; (**b**) detail at 500×.

3.8. Attack 8—Klemm Reagent

When the Ni-hard alloy is attacked with Klemm reagent, the austenite is colored light brown, the martensite remains white and the pearlite is darkened. The eutectic carbides are not dyed by Klemm reagent (Figure 8).

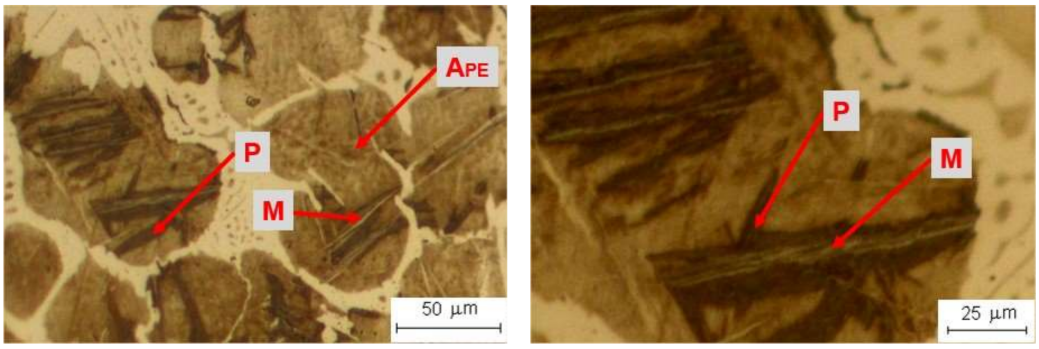

(**a**) (**b**)

Figure 8. Klemm reagent: (**a**): general view at 200×; (**b**) detail at 500×.

3.9. Attack 9—Nital-3 at Room Temperature

Nital-3 is traditionally used for ferrous alloys and darkens the ferrite grain boundaries and the interface between ferrite and cementite. After its attack, the austenite is distinguished in a light brown tone, the pearlite is darkened, and the martensite and the eutectic carbides remain white. The secondary carbides cannot be distinguished from any other carbides (Figure 9).

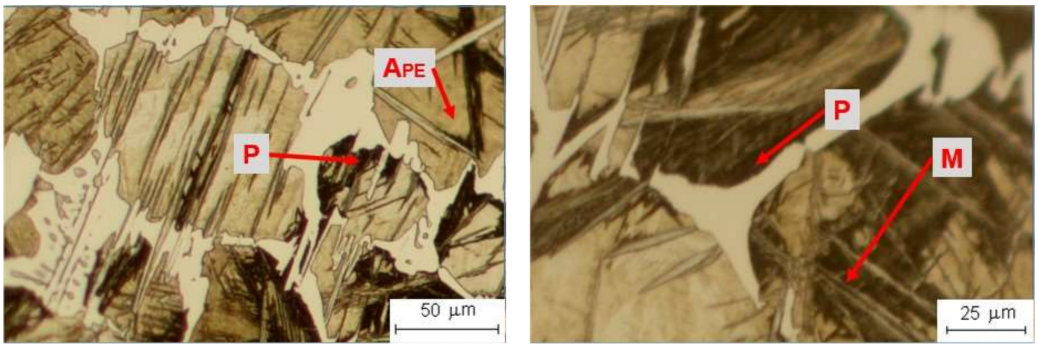

(**a**) (**b**)

Figure 9. Nital-3 at room temperature: (**a**) general view at 200×; (**b**) detail at 500×.

3.10. Attack 10—Marble Reagent at Room Temperature

The Marble reagent does not attack the matrix of eutectic carbides. However, it turns the proeutectic austenite grains in brown tones and pearlite in almost black tones. Martensite appears as white needles. Also, white areas are observed inside the proeutectic grains, resembling the secondary carbides already seen with Kalling N°1 (Figure 10).

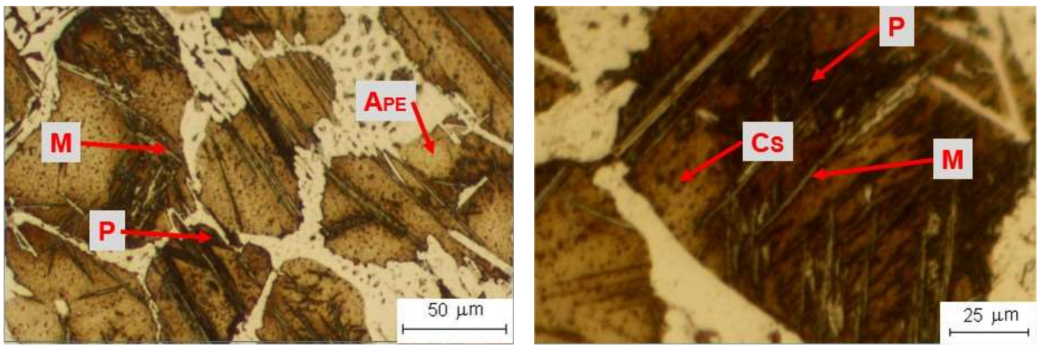

(**a**) (**b**)

Figure 10. Marble reagent at room temperature: (**a**) general view at 200×; (**b**) detail at 500×.

3.11. Attack 11—Picral Reagent

The Picral attack also induces a difference of tonality between the pearlitic and martensitic microconstituents. Austenite grains are darkened whereas the eutectic carbide matrix remains unaltered. Martensite and pearlite have also been attacked, as the pearlite has darker shades (Figure 11).

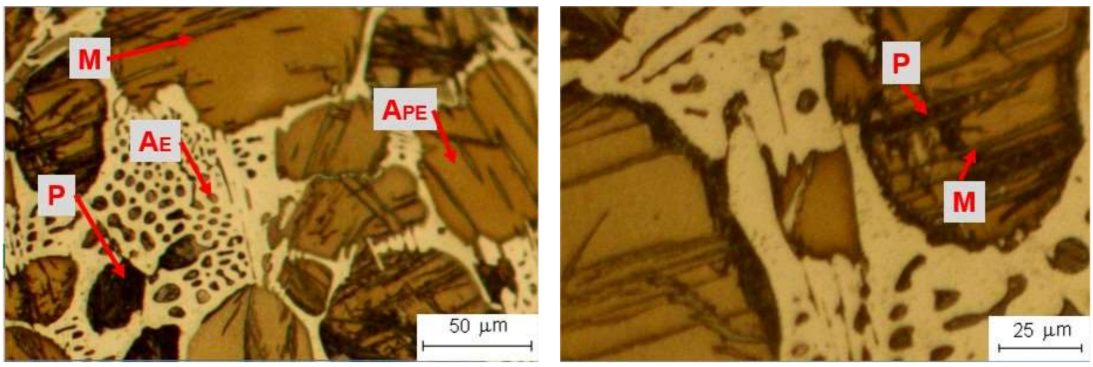

(**a**) (**b**)

Figure 11. Picral reagent: (**a**) general view at 200×; (**b**) detail at 500×.

3.12. Attack 12—Vilella Reagent for 20 s

The Vilella reagent hardly attacks the phases of the white cast. There is a black-colored phase corresponding to martensite with their characteristic morphology in needles, forming 60° between them. Areas with a darker hue are also observed, which corresponds to the matrix of eutectic carbides (Figure 12).

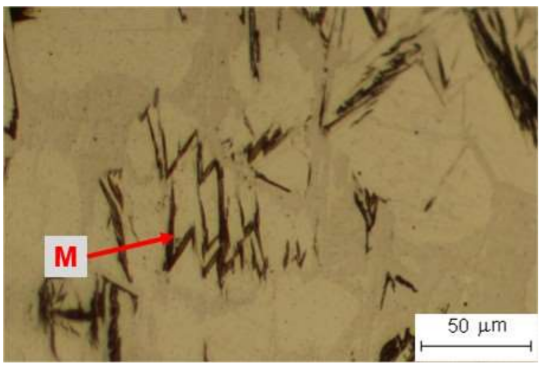

Figure 12. Vilella reagent for 20 s, (200×).

4. Discussion

The results of the described attacks are summarized in Table 2. It is seen that it is possible to distinguish all the microconstituents present in the Ni-Hard alloy studied, including those that are not usually distinguishable with the typical reagents [1,26,38,40]. Considering the importance of the carbide matrix for the wear applications of these alloys [8,18], Table 2 should be used to identify them. Afterward, through image analysis, for instance, the rates between the microconstituents can be related to the measured hardness. For metallurgical purposes, the most interesting case is the possibility of distinguishing between pearlite and martensite, feasible through attack 12. Even though this differentiation is feasible through microscopy—the lamellar structure of the pearlite and the needles of martensite are observable through SEM [17,21,45,46], for instance, or chemical analysis, EDX or EDMA analysis may point out that pearlite has a narrower range of carbon contents [47]—it is not easy to discriminate between them through metallographic techniques [48].

To identify the austenite, the etchant combination of attack 4 is the best choice, coloring it to a blue shade. To selectively attack the eutectic carbides, attack 7 darkens them, as well as the intragranular carbides.

Table 2. Microconstituents status after each attack studied (APE: Proeutectic austenite; AE: Eutectic austenite; M: martensite; P: pearlite; CE: eutectic carbides; CS: secondary carbides; RT: room temperature; HT: high temperature; Cont.: contoured).

Attack				Microconstituent					
#	**Reagent**	**t (s)**	**Temp**	**APE**	**AE**	**M**	**P**	**CE**	**CS**
1	Marshall	5	RT	Cont.	Cont.	No	Slightly	Cont.	No
2	Marshall	25	RT	Cont.	Cont.	Slightly	Dark	Cont.	No
3	Marshall	60	RT	Cont.	Cont.	Slightly	Dark	Cont.	No
4	Attack 3 + 5% ammonium persulfate	25	RT	Blue	Blue	Dark	Dark	Cont.	Cont.
5	Attack 4 + Kalling N°1	60	RT	Slightly	Dark	Dark	Dark	Cont.	Cont.
6	Murakami	60	HT	No	No	Dark	Dark	Gray	Gray
7	Murakami	60	RT	No	No	No	No	Dark	Gray
8	Klemm	20	RT	Slightly	Slightly	No	Dark	No	No
9	Nital-3	40	RT	Slightly	Slightly	No	Dark	No	No
10	Marble	10	RT	Slightly	Dark	No	Dark	No	Cont.
11	Picral	10	RT	Slightly	Slightly	Slightly	Dark	No	No
12	Vilella	20	RT	No	No	Dark	No	Slightly	No

5. Conclusions

The objective of this paper is to identify the type, morphology, distribution, and quantity of microconstituents with selective reagents, regarding the influence on the behavior in service of the Ni-hard white cast iron. Different reagents have been chosen from those proposed in the literature to reveal each one of the microconstituents. Although the most common choice for this type of castings, ferrous alloys, is the Nital-3 or Picral reagents, it is clear in this study the need to use other reagents to unambiguously reveal the appearing microconstituents. There are several possible etchants to identify the microstructure of these alloys, regarding specific microconstituent that is wanted to be spotted. In Table 2, the comparison of all attacks made to the Ni-Hard cast iron is shown. All the possible microconstituents, as well as their arrangement, are thus identified just by observing the microstructure of the alloy. Among the studied attacks, the best selection for each relevant microconstituent—pearlites and bainites have been excluded—is displayed in Table 3.

Table 3. Attack selection for each microconstituent present in Ni-hard alloys.

Microconstituent	Attack
M: Martensite	12: Vilella reactant
APE: Proeutectic austenite	4: Marshall + 5% ammonium persulfate
CE: Eutectic carbides	7: Murakami reactant
CS: Secondary carbides	7: Murakami reactant

Owing to its common applications, the most important microconstituent is the carbide matrix, but the rate between hard and soft components should be also studied. Thus, the proeutectic austenite, the eutectic carbides, the martensite, and the pearlite must be identified. As said before, high quantity martensite or carbides show better behavior against wear, whereas the austenite improves its tenacity. As the proportion between these constituents can be controlled through the fabrication of the alloy [49,50], it allows determining errors in this process.

Author Contributions: Conceptualization, M.G.F.d.C.; methodology, M.G.F.d.C. and B.d.R.; validation, J.J.M.-L. and M.P.-L.; formal analysis, Y.M.Á.; writing—original draft preparation, M.G.F.d.C.; writing—review and editing, J.J.M.-L. and M.P.-L.; supervision, M.G.F.d.C. All authors have read and agreed to the published version of the manuscript.

Funding: This research received no external funding.

Conflicts of Interest: The authors declare no conflict of interest.

References

1. Jiyang, Z. Colour Metallography of Cast Iron. *China Foundry* **2009**, *6*, 57–69. Available online: http://caod.oriprobe.com/articles/15277740/zhonggzz090111.htm (accessed on 30 May 2020).
2. *ASTM E407-07 (2015) e1, Standard Practice for Microetching Metals and Alloys*; ASTM International: West Conshohocken, PA, USA, 2015.
3. Bailey, A.R.; Samuels, L.E. *Foundry Metallography*; Metallurgical Services: Betchworth, UK, 1971.
4. Pero-Sanz, J.A.; Plaza, D.; Verdeja, J.I.; Asensio, J. Metallographic Characterization of Hypoeutectic Martensitic White Cast Irons: Fe-C-Cr System. *Mater. Charact.* **1999**, *43*, 33–39. [CrossRef]
5. Vander Voort, G.F. Metallography and Microstructures of Cast Iron. In *ASM Handbook, Volume 09—Metallography* and Microstructures; ASM International: Materials Park, OH, USA, 2004; p. 2.
6. UNE. UNE-EN 12513:2011 Fundición: Fundiciones Resistentes a la Abrasión. 2011. Available online: https://www.une.org/encuentra-tu-norma/busca-tu-norma/norma?c=N0048185 (accessed on 30 May 2020).
7. Kopyciński, D.; Piasny, S.; Kawalec, M.; Madizhanova, A. The Abrasive Wear Resistance of Chromium Cast Iron. *Arch. Foundry Eng.* **2014**, *14*, 63–66. [CrossRef]
8. Pokusová, M.; Berta, I.; Šooš, L. Abrasion Resistance of as-Cast High-Chromium Cast Iron. *Sci. Proc. Fac. Mech. Eng.* **2014**, *22*, 75–80. [CrossRef]
9. Álvarez Antolín, J.F.; Asensio Lozano, J.; Álvarez Pérez, C.H. Identification of Metallurgical Manufacturing Factors with a Significant Effect on the Flexural Strength of Mottled Ni-Hard Cast Irons Through a Design of Experiments Approach. *Int. J. Met.* **2017**, *11*, 467–474. [CrossRef]
10. Flórez, O.E.; Castaño, R.A.; Higuera, O.F. Comportamiento microestructural de una fundición blanca al alto cromo sometida a ciclos de tratamientos térmicos. *Sci. Tech.* **2010**, *16*, 43–48. Available online: http://www.redalyc.org/articulo.oa?id=84917249008 (accessed on 30 May 2020).
11. Gelfi, M.; Pola, A.; Girelli, L.; Zacco, A.; Masotti, M.; La Vecchia, G.M. Effect of heat treatment on microstructure and erosion resistance of white cast irons for slurry pumping applications. *Wear* **2019**, *428–429*, 438–448. [CrossRef]
12. Matsubara, Y.; Sasaguri, N.; Yokomizo, Y.; Hashimoto, M. Influence of carbon content on phase transformation characteristics of multi-component white cast iron for mill materials. *Int. J. Cast Met. Res.* **2003**, *16*, 77–82. [CrossRef]
13. Matsubara, Y. *Research and Development of Abrasion Wear Resistant Cast Alloys for Rolls of Rolling and Pulverizing Mills*; Kurume National College of Technology: Kurume, Japan, 2002; Available online: http://203.187.160.133:9011/www.hwe.oita-u.ac.jp/c3pr90ntc0td/kiki/ronnbunn/paper_matubara.pdf (accessed on 30 May 2020).
14. Ramos, Y. *Fabricación de Bolas Para Molinos Por Fundición de Hierro Aleado Ni-Hard*; Instituto Superior Minero Metalúrgico: Moa, Cuba, 2017; Available online: http://ninive.ismm.edu.cu/handle/123456789/2552 (accessed on 30 May 2020).
15. Filipovic, M.; Kamberovic, Z.; Korac, M. Solidification of High Chromium White Cast Iron Alloyed with Vanadium. *Mater. Trans.* **2011**, *52*, 386–390. [CrossRef]
16. González, M. *Apuntes de Fundiciones Férreas Aleadas, Sección de Publicaciones de la E.T.S*; Ingenieros Industriales: Madrid, Spain, 2006.
17. Alamdarlo, M.B.; Amini, K.; Najafabadi, V.N.; Mohammadnezhad, M. Investigating the Effect of Titanium Addition on the Microstructure and Mechanical Properties of Ni-Hard 4 Cast Iron. *J. Mod. Process. Manuf. Prod.* **2016**, *5*, 17–27.
18. Wiengmoon, A. Carbides in High Chromium Cast Irons. *Naresuan Univ. Eng. J.* **2011**, *6*, 64–71. [CrossRef]

19. Guitar, M.A.; Scheid, A.; Suárez, S.; Britz, D.; Guigou, M.D.; Mücklich, F. Secondary carbides in high chromium cast irons: An alternative approach to their morphological and spatial distribution characterization. *Mater. Charact.* **2018**, *144*, 621–630. [CrossRef]
20. Dogan, O.N.; Hawk, J.A.; Rice, J. Comparison of three Ni-Hard I alloys. In Proceedings of the TMS (The Minerals, Metals and Materials Society), Warrendale, PA, USA, 1 September 2004.
21. Chen, L.; Zhou, J.; Bushlya, V.; Stahl, J. Influences of Micro Mechanical Property and Microstructure on Performance of Machining High Chromium White Cast Iron with cBN Tools. *Procedia CIRP* **2015**, *31*, 172–178. [CrossRef]
22. Baiuk, A. Studies of a wear resistant cast iron. *Metal. J. Metall.* **2003**, *9*, 259–272.
23. Vander Voort, G.F. *Applied Metallography*; Van Nostrand Reinhold: New York, NY, USA, 1986.
24. *ASM Handbook*; ASM International: Materials Park, OH, USA, 2004; Volume 9.
25. Vander Voort, G.F. *Metallography*, 1st ed.; ASM: Materials Park, OH, USA, 1999.
26. Mehranfar, S.; Ghasemi Banadkouki, S.S.; Kallantar, M.; Mosallepour Yazdi, M. Improved Color Metallography for a Low Alloy Hardened White Cast Iron. *ISIJ Int.* **2012**, *52*, 1649–1654. [CrossRef]
27. Davis, J.R. *Cast Irons*, 1st ed.; ASM International: Materials Park, OH, USA, 1996.
28. Ni-Hard. Material Data and Applications. Available online: https://nickelinstitute.org/media/1728/ni_hardmaterialdataandapplications_11017_.pdf (accessed on 29 January 2020).
29. Ni-Hard Compositions. Available online: http://www.funcasa-mein.com/en/descargas/ni_hard.pdf (accessed on 12 May 2020).
30. Bahfie, F.; Nurjaman, F.; Lisa, F.I. Syafriadi Effect of vanadium on the mechanical properties and microstructure of Ni-Hard 2. *AIP Conf. Proc.* **2020**, *2232*, 060003. [CrossRef]
31. Mancera, W.F.; Sanabria, J.M. *Estudio de la Influencia del Vanadio en la Resistencia a la Corrosión y al Desgaste en una Aleación Ni-Hard*; Universidad Libre de Colombia: Bogotá, Colombia, 2017.
32. Mourad, M.; El-Hadad, S.; Ibrahim, M. Effects of Molybdenum Addition on the Microstructure and Mechanical Properties of Ni-Hard White Cast Iron. *Trans. Indian Inst. Met.* **2015**, *68*, 715–722. [CrossRef]
33. Wieczerzak, K.; Bala, P.; Stepien, M.; Cios, G.; Koziel, T. Formation of eutectic carbides in Fe–Cr–Mo–C alloy during non-equilibrium crystallization. *Mater. Des.* **2016**, *94*, 61–68. [CrossRef]
34. Kadhim, M.J.; Abood, A.N.; Yaseen, R.S. The Role of Manganese on Microstructure of High Chromium White Cast Iron. *Mod. Appl. Sci.* **2011**, *5*, 179. [CrossRef]
35. Çöl, M.; Koç, F.G.; Öktem, H.; Kır, D. The role of boron content in high alloy white cast iron (Ni-Hard 4) on microstructure, mechanical properties and wear resistance. *Wear* **2016**, *348–349*, 158–165. [CrossRef]
36. Murakami, T. On the Structure of Iron-Carbon-Chromium Alloys. *Sci. Rep.* **1918**, *7*, 217.
37. Klemm, H. *Color Etching of the Fine Structure of Metals with Sodium Thiosulfate*; MetallkundlicheVerlag Technik Berlin: Berlin, Germany, 1952; Volume 45.
38. Klemm, H. Uses of Sodium Thiosulfate (Klemm's Reagent) as an Etchant. *Prakt. Metallogr.* **1968**, *5*, 163.
39. Osborne, A.K. *An Encyclopaedia of the Iron & Steel Industry*; The Technical. Pr: London, UK, 1956.
40. Benscoter, A.; Perricone, M. Marshall's Reagent: Origins, Modifications, and New Applications. *Microsc. Microanal.* **2005**, *11*, 76–77. [CrossRef]
41. Rawdon, H.S. *Use of Ammonium Persulphate for Revealing the Macrostructure of Iron and Steel*; Government Printing Office: Washington, DC, USA, 1920.
42. Bramfitt, B.L. *Metallographer's Guide: Practices and Procedures for Irons and Steels*; ASM International: Materials Park, OH, USA, 2001.
43. Vander Voort, G. Color Metallography. *Microsc. Microanal.* **2004**, *10*, 70–71. [CrossRef]
44. Zipperian, D.C. *Metallographic Handbook*; PACE Technologies: Tucson, AZ, USA, 2011.
45. Hamada, S.; Sasaki, D.; Ueda, M.; Noguchi, H. Fatigue limit evaluation considering crack initiation for lamellar pearlitic steel. *Procedia Eng.* **2011**, *10*, 1467–1472. [CrossRef]
46. Navarro-López, A.; Hidalgo, J.; Sietsma, J.; Santofimia, M.J. Characterization of bainitic/martensitic structures formed in isothermal treatments below the Ms temperature. *Mater. Charact.* **2017**, *128*, 248–256. [CrossRef]
47. Li, Z.R.; Li, Z. *Industrial Applications of Electron Microscopy*; CRC Press Inc.: Baton Rouge, LA, USA, 2003.
48. Blázquez, V.M. *Metalografía de las Aleaciones Férreas, Sección de Publicaciones de la E.T.S*; Ingenieros Industriales: Madrid, Spain, 1991.

49. Rizov, B. Some Results from the Investigation of Effects of Heat Treatment on Properties of Ni-Hard Cast Irons. *Int. J. Eng. Res. Dev.* **2017**, *13*, 30–35.
50. Kopyciński, D.; Guzik, E.; Siekaniec, D.; Szczęsny, A. Analysis of the High Chromium Cast Iron Microstructure after the Heat Treatment. *Arch. Foundry Eng.* **2014**, *14*, 43–46. [CrossRef]